

Assessment of Anticancer Properties of Synthesized Pyrazole-Acridine Derivative on SH-SY5Y Human Neuroblastoma Cells

Sentezlenen Pirazol-Akridin Türevinin SH-SY5Y İnsan Nöroblastoma Hücrelerinde Antikanser Özelliklerinin Değerlendirilmesi

Yusuf KÜÇÜKBAĞRIACIK¹

0000-0002-4909-2669

Muna ELMUSA²

0000-0003-4087-4944

Fatma ELMUSA³

0000-0001-6645-5487

Hümeysra YILMAZ⁴

0000-0001-7530-4568

Rahmi KASIMOĞULLARI⁵

0000-0001-6391-7121

Mohammadreza DASTOURI⁴

0000-0003-3882-0728

¹Department of Biophysics, Health Sciences University Gülhane Faculty of Medicine, Ankara, Türkiye

²Elfurat Engineering Research and Development Limited Company, Ankara, Türkiye

³Department of Molecular Biology, Eskisehir Technical University Institution of Graduate Schools, Eskisehir, Türkiye

⁴Department of Medical Biology, Ankara Medipol University School of Medicine, Ankara, Türkiye

⁵Department of Chemistry, Dumlupınar University Faculty of Art and Science, Kütahya, Türkiye

Corresponding Author

Sorumlu Yazar

Yusuf KÜÇÜKBAĞRIACIK

yusuf.kucukbagriacik@sbu.edu.tr

Received / Geliş Tarihi : 23.07.2024

Accepted / Kabul Tarihi : 02.01.2025

Available Online /

Çevrimiçi Yayın Tarihi : 31.01.2025

ABSTRACT

Aim: This study aimed to synthesize a novel pyrazole acridine derivative (3-ACH) and evaluate its anticancer properties on SH-SY5Y human neuroblastoma cells.

Material and Methods: The pyrazole-4-carbaldehyde derivative was cyclized with dimedone and p-nitroaniline to synthesize the 3-ACH. Characterization of the compound was performed using FT-IR, NMR, HPLC-Q-TOF/MS, and elemental analysis. The cytotoxic impact of the 3-ACH compound on SH-SY5Y human neuroblastoma cells was evaluated using the WST-1 assay in a dose- (50, 100, and 150 µg/mL) and time-dependent (12, 24, and 48 hours) manner. The impact of 3-ACH on apoptosis was investigated through immunostaining for Caspase-3, -8, and -9, and BAX proteins.

Results: 3-ACH reduced SH-SY5Y cell viability with the rate of 89.89±7.63% (p=0.002) at 100 µg/mL concentration after 24 hours of treatment. While a higher (150 µg/mL) concentration showed a similar reduction (90.53±2.88%, p=0.004), the lower (50 µg/mL) concentration maintained high cell viability (98.37±1.67%, p=0.903) at 24 hours. All doses of 50 µg/mL (94.55±0.65%), 100 µg/mL (95.18±1.41%), and 150 µg/mL (95.28±2.57%) significantly reduced cell viability rates, at 48 hours (all p<0.001). Immunostaining revealed a significant upregulation in the synthesis of BAX, Caspase-3, -8, and -9 proteins in cells treated with 3-ACH (100 µg/mL) for 24 hours compared to the control group.

Conclusion: These results indicate that 3-ACH has the potential to induce apoptosis in SH-SY5Y cells by activating both the intrinsic and extrinsic pathways, which may contribute to its cytotoxic effects. This study provides promising evidence supporting the potential of the 3-ACH compound as an anticancer therapeutic agent.

Keywords: Chemical synthesis; antineoplastic agents; neuroblastoma; pyrazoles; acridines; cytotoxicity; apoptosis.

ÖZ

Amaç: Bu çalışmanın amacı yeni bir pirazol akridin türevi (3-ACH) sentezlemek ve bu bileşiğin SH-SY5Y insan nöroblastoma hücreleri üzerindeki antikanser özelliklerini değerlendirmektir.

Gereç ve Yöntemler: Pirazol-4-karbaldehit türevi, 3-ACH sentezlemek için dimedon ve p-nitroanilin ile siklize edildi. Bileşiğin karakterizasyonu FT-IR, NMR, HPLC-Q-TOF/MS ve element analizi kullanılarak yapıldı. 3-ACH bileşiğinin SH-SY5Y insan nöroblastoma hücreleri üzerindeki sitotoksik etkisi, doz (50, 100 ve 150 µg/mL) ve zaman (12, 24 ve 48 saat) bağımlı bir şekilde WST-1 testi kullanılarak değerlendirildi. 3-ACH'nin apoptoz üzerindeki etkisi, Kaspaz-3, -8, -9 ve BAX proteinleri için immün boyama yolu ile araştırıldı.

Bulgular: 3-ACH, 100 µg/mL konsantrasyonda 24 saatlik tedaviden sonra SH-SY5Y hücre canlılığını %89,89±7,63 (p=0,002) oranında azaltmıştır. 24 saatte, daha yüksek (150 µg/mL) konsantrasyon benzer bir azalma gösterirken (%90,53±2,88, p=0,004), daha düşük (50 µg/mL) konsantrasyon hücre canlılığını korumuştur (%98,37±1,67, p=0,903). 50 µg/mL (%94,55±0,65), 100 µg/mL (%95,18±1,41) ve 150 µg/mL (%95,28±2,57) dozlarının tümü, 48 saatte hücre canlılık oranlarını önemli ölçüde azaltmıştır (tüm p<0,001). İmmün boyama, 24 saat boyunca 3-ACH (100 µg/mL) ile muamele edilen hücrelerde, BAX, Kaspaz-3, -8 ve -9 proteinlerinin sentezinde kontrol grubuna kıyasla önemli bir artış olduğunu ortaya koymuştur.

Sonuç: Bu sonuçlar, 3-ACH'nin hem intrinsik hem de ekstrinsik yolları aktive ederek SH-SY5Y hücrelerinde, sitotoksik etkilerine katkıda bulunabilecek olan, apoptozu indüklemeye potansiyeline sahip olduğunu göstermektedir. Bu çalışma, 3-ACH bileşiğinin antikanser terapötik ajan olarak potansiyelini destekleyen umut verici kanıtlar sunmaktadır.

Anahtar kelimeler: Kimyasal sentez; antineoplastik ajanlar; nöroblastoma; pirazoller; akridinler; sitotoksikite; apoptoz.

INTRODUCTION

Pyrazole is a 5-membered organic heterocyclic compound containing nitrogen and carbon atoms, with the chemical formula $C_3H_3N_2$ (1). The pyrazole ring closely resembles the imidazole compound, but with the substitution of a nitrogen atom by a carbon atom. Pyrazole and its derivatives have been reported to be present in various natural products (2). Due to the chemical diversity of pyrazoles, they have been extensively investigated and found to exhibit various pharmacological properties, including anti-inflammatory, anti-cancer, anti-viral, and anti-bacterial effects (3). Moreover, certain pyrazoles have exhibited inhibitory properties against cancer cell proliferation, positioning them as viable candidates for anti-tumor agents (4). Additionally, there is a need to explore innovative strategies to optimize the side effect profile, pharmacokinetics, and pharmacodynamics of pyrazoles (5), including enhancing pyrazole activity, reducing toxicity, and increasing water solubility (6,7).

Acridine is a heterocyclic compound belonging to the class of organic compounds known as polycyclic aromatic hydrocarbons (8). Its unique molecular structure has attracted significant attention, leading to extensive investigations regarding its potential applications in various fields. Acridine and its derivatives have been the subject of numerous studies due to their interactions with DNA and RNA, notable fluorescence properties, and enzyme inhibition capabilities, particularly against topoisomerases (9). The intercalation of acridine with DNA is believed to underlie its anticancer activity, as it can disrupt DNA replication and induce cell death (10). Encouraging results have emerged from preclinical and clinical trials, demonstrating the efficacy of acridine-based drugs in inhibiting tumor growth and achieving successful cancer treatment across various types, including breast, lung, and colon cancers.

Pyrazoloacridine, a compound that combines acridine with the pyrazole ring, belongs to the class of anthrapyrazoles, which have shown antitumor activity similar to doxorubicin but with reduced cardiotoxicity (11,12). It has been extensively studied *in vitro* and *in vivo* against various cancer types, particularly leukemia, and has demonstrated promising effectiveness (12).

While various pyrazole-acridine derivatives have been investigated for their biological activities, the specific compound 9-(1-(benzo[d]thiazol-2-yl)-3-(4-chlorophenyl)-1H-pyrazol-4-yl)-3,3,6,6-tetramethyl-10-(4-nitrophenyl)-3,4,6,7,9,10-hexahydroacridine-1,8(2H,5H)-dione (3-ACH) represents a novel molecular entity that was first synthesized by Elmusa et al. (13). Their initial study focused exclusively on the compound's acetylcholinesterase inhibitory properties through *in vitro* and *in silico* approaches. However, the potential anticancer properties of 3-ACH, particularly against neuroblastoma cells, have not been previously investigated. The unique structural features of 3-ACH, including the benzothiazole moiety and the specific substitution pattern of the pyrazole-acridine scaffold, distinguish it from other previously reported pyrazole-acridine derivatives. This structural novelty, combined with the unexplored anticancer potential, presents an opportunity to evaluate 3-ACH as a potential therapeutic agent against neuroblastoma, thereby expanding the understanding of structure-activity relationships in this class of compounds.

In this study, the goal was to develop new agents with improved anticancer activity by integrating pyrazole and acridine, which individually exhibit anticancer properties, within a single molecule. To achieve this, hydrazone synthesis was initially conducted, followed by the synthesis of the compound referred to as 1-(benzo[d]thiazol-2-yl)-3-(4-chlorophenyl)-1H-pyrazole-4-carbaldehyde (P4C) using the hydrazone as a precursor. Subsequently, cyclization of the synthesized pyrazole-4-carbaldehyde was accomplished by utilizing dimedone and *p*-nitroaniline, leading to the formation of 3-ACH, the pyrazole-acridine derivative. Following synthesis, the obtained pyrazole-acridine derivative was subjected to characterization using FT-IR, NMR, HPLC-Q-TOF/MS, and elemental analysis techniques. Subsequently, the anticancer activity of the obtained pyrazole-acridine derivative was tested against the SH-SY5Y neuroblastoma cell line. Test concentrations of 50, 100, and 150 $\mu\text{g/mL}$ were employed, and the assessment was conducted over incubation durations of 12, 24, and 48 hours. The WST-1 assay was employed to evaluate the cytotoxic impact of the pyrazole-acridine derivative on the SH-SY5Y cell line. Additionally, immunostaining techniques were employed to evaluate the expression levels of proteins associated with the apoptotic pathway, including Caspase-3, -8, and -9, and BAX. These investigations aimed to provide insights into the apoptotic mechanism of 3-ACH on human neuroblastoma cancer cell lines.

MATERIAL AND METHODS

Chemical Synthesis

The chemicals used in this study were obtained from Sigma, Aldrich, Fluka, and Merck companies. The solvents employed were distilled prior to use. All compounds are >95% pure by HPLC analysis. The synthesis of the pyrazole-acridine derivative was performed in two stages. In the first stage, the hydrazone compound was synthesized by employing 4-chloroacetophenone and 2-hydrazinobenzothiazole as precursors. Subsequently, the Vilsmeier-Haack reagent was introduced to the hydrazone compound to facilitate the synthesis of P4C, which served as the initial compound containing the benzothiazole moiety. In the second stage, the synthesized P4C was activated through its reaction with dimedone and *p*-nitroaniline, resulting in the conversion to the desired pyrazole-acridine derivative, 3-ACH.

For the synthesis of 2-(2-(1-(4-chlorophenyl)ethylidene)hydrazino)benzo[d]thiazole compound, 1 g (6 mmol) of 2-hydrazinobenzothiazole and 0.94 g (6 mmol) of 4-chloroacetophenone were mixed in a flask and dissolved in 20 mL of ethanol. Subsequently, 0.4 mL of acetic acid was added to the mixture, which was then refluxed for 3 hours. The resulting beige precipitate was washed with a 2:1 mixture of water and ethanol, followed by purification through crystallization in butanol.

For the synthesis of P4C, 0.55 mL (6 mmol) of phosphoryl chloride (POCl_3) was kept in an ice bath for 20 minutes, and then 2 mL of cooled *N,N*-dimethylformamide (DMF) was added dropwise. After stirring for a few minutes, 0.301 g (1 mmol) of the compound 2-(2-(1-(4-chlorophenyl)ethylidene)hydrazino)benzo[d]thiazole was added to the mixture. The reaction mixture was stirred in an ice bath for

30 minutes, followed by an additional 30 minutes at room temperature. It was subsequently refluxed in an oil bath at 80-90 °C for 5 hours. After cooling the mixture to room temperature, ice water was added, resulting in the formation of a brown precipitate, which was further purified by crystallization from toluene.

To synthesize 3-ACH, a solution was prepared by dissolving 0.340 g (1 mmol) of P4C and 0.019 g (0.1 mmol) of p-toluenesulfonic acid (TSA) in 10 mL of tetrahydrofuran (THF). 0.280 g (2 mmol) of dimedone was added to this solution and stirred for 5 minutes. Next, 0.138 g (1 mmol) of p-nitroaniline was introduced into the solution, followed by refluxing for 6 hours. The resultant yellow precipitate was washed with water and further purified through crystallization from ethanol (13).

Characterization

DC-Alufolien 20x20 cm Kieselgel 60 F254 analytical thin-layer chromatography (TLC) plates and a Camag UV lamp (254-366 nm) were utilized to monitor the progress of the reactions conducted in this study. The melting points of the synthesized compounds were measured using the Barnstead Electrothermal 9200 instrument. Fourier-transform infrared spectroscopy (FT-IR) was conducted using the Bruker Optics Vertex 70 instrument, providing valuable information about the functional groups present in the compounds. High-performance liquid chromatography quadrupole time-of-flight mass spectrometry (HPLC-Q-TOF/MS) was performed using the Agilent 1260 infinity HPLC system coupled with a 6210 time of flight (TOF) LC/MS detector to analyze the mass of the synthesized compounds. Nuclear magnetic resonance (NMR) spectroscopy was employed for detailed structural analysis, with ¹H-NMR analysis conducted at 600 MHz and ¹³C-NMR analysis at 150 MHz. In NMR analyses, CDCl₃ was used as the solvent, providing a chemical shift reference of 7.26 ppm for ¹H-NMR and 77.2 ppm for ¹³C-NMR. Finally, elemental analysis of the compounds was performed using the Leco CHNS-932 device (13).

Sample Size

Sample size calculation was performed using G*Power software v.3.1.9.7. For one-way ANOVA comparison between groups with $\alpha=0.05$, power $(1-\beta)=0.80$, effect size $f=0.6$, and four experimental groups (one control and three treatment groups), the minimum required total sample size was calculated as 36 (9 samples per group). In our experimental design, we conducted six independent biological replicates for each group, with each replicate consisting of three technical replicates, resulting in a total of 18 measurements per group. This sample size exceeded the minimum requirement, achieving an actual statistical power of 0.82, which ensured robust statistical analysis of the experimental data.

Cell Culture

The SH-SY5Y human neuroblastoma cell line (ATCC® CRL-2266™) was cultured in DMEM high glucose medium (Sigma-D6429-500 ML), supplemented with 10% heat-inactivated fetal bovine serum (Biowest, S181H-500), 1% L-glutamine (Gibco, 25030081), and 1% penicillin-streptomycin (Gibco, 10378016). The cells were kept in a 37 °C incubator with 5% CO₂, and observations related to cell viability and growth rates were conducted using a microscope.

Study Design and Experimental Groups

The study was designed to evaluate both the dose- and time-dependent effects of 3-ACH on SH-SY5Y human neuroblastoma cells. The experimental design consisted of four groups: a control group (0.1% DMSO) and three treatment groups receiving different concentrations of 3-ACH (50, 100, and 150 µg/mL). These concentrations were selected based on our previous study where these doses showed significant cytotoxic effects against SKBR-3 human breast cancer cells (14). Time points (12, 24, and 48 hours) were chosen to evaluate both early and late effects of the compound. Cell viability was assessed using WST-1 assay and expressed as a percentage of viable cells relative to control (100%). For apoptosis-related protein expression studies, the 24-hour time point and 100 µg/mL concentration were selected based on the optimal cytotoxic response observed in viability assays. Each experiment was performed with six independent biological replicates per group.

Cell Viability/Cytotoxicity Assay (WST-1)

The WST-1 assay is used to assess cell viability and cytotoxicity. In this study, we employed the WST-1 to evaluate the cytotoxic effects of different doses and durations of 3-ACH administration on human neuroblastoma cells. To assess the anticancer potential of 3-ACH, we conducted cell viability measurements using the WST-1 assay (Takara Premix WST-1 Cell Proliferation Assay System MK400), following the manufacturer's guidelines. The assay is based on the conversion of tetrazolium salt into formazan by mitochondrial dehydrogenases within the cells. Stock solutions of the tested compounds were diluted in complete medium to final concentrations of 50, 100, and 150 µg/mL. The cells were exposed to various concentrations of the compounds or a maximum vehicle dose (0.1% DMSO). After incubation periods of 12, 24, and 48 hours, cell viability was assessed. The cells were treated with the WST-1 reagent and incubated for 4 hours at 37 °C. Absorbance was then measured at 450 nm using a microplate reader (Tecan Infinite 200pro) (15).

Immunostaining

Immunostaining is a technique that depends on the creation of antigen-antibody complexes. In this study, we employed immunostaining to investigate the apoptotic pathways activated in SH-SY5Y cells following the administration of 3-ACH. The aim was to elucidate the process of cell death associated with apoptosis using this methodology. Based on cytotoxicity results, SH-SY5Y cells were treated with 3-ACH at 100 µg/mL for 24 hours. The cells cultured on coverslips were fixed with a 3.5% paraformaldehyde solution (Sigma-158127). After fixation, the cells were rinsed with PBS (Gibco, 14190-094) and immersed in PBS azide (Chemcruz, SC-296028). The fixed cells were incubated individually with primary antibodies against BAX (Abcam, ab32503, rabbit), Caspase-3 (Abcam, ab13847, rabbit), Caspase-8 (Abcam, ab32125, rabbit), and Caspase-9 (Abcam, ab202068, rabbit) for 24 hours at +4 °C. Subsequently, the coverslips were washed twice with PBS to remove unbound antibodies. The cells were then treated with FITC-labeled secondary antibody (Sigma, F9887, anti-rabbit) for 2 hours at 37 °C. Following another round of PBS washing, the cells were stained with 7-amino actinomycin D (7-AAD), a DNA dye, for 30 minutes at 37 °C (15).

Cell nuclei were stained with 7-AAD dye, producing a red signal, while target proteins were labeled with a FITC-conjugated antibody, emitting a green signal. The intensity of these signals was analyzed using ImageJ software, and the images of nuclei and cytoplasm were merged. Immunofluorescence images were qualitatively evaluated by visually comparing fluorescence signals between the control and treatment groups.

The immunostained cells were visualized and photographed using an inverted fluorescence microscope (ZEISS Axioscope 5) equipped with appropriate filter sets for FITC (excitation: 495 nm/emission: 519 nm) and 7-AAD (excitation: 546 nm/emission: 647 nm). Representative images were captured at 100X magnification. The green fluorescence (FITC signal) indicated the presence and relative expression levels of target proteins (BAX, Caspase-3, -8, and -9), while the red fluorescence (7-AAD) showed nuclear staining. The relative protein expression levels were evaluated by comparing the intensity of green fluorescence between control and treated groups in representative fields. An increase in green fluorescence intensity indicated elevated protein expression compared to control cells.

Ethics Statement

This study utilized commercially available cell lines and did not involve human subjects or animal experiments. Therefore, ethics committee approval was not required.

Statistical Analysis

Statistical analysis of cytotoxicity data obtained in the study was performed using IBM SPSS Statistics Version 27.0 software. Data normality was assessed using the Shapiro-Wilk test, and homogeneity of variances was evaluated using the Levene test. One-way ANOVA followed by Tukey's post-hoc test was used for multiple comparisons. Results are expressed as mean±standard deviation. Statistical significance was determined at a threshold of $p < 0.05$ for all results.

RESULTS

The synthesis of the pyrazole-acridine derivative was completed in two stages (Figure 1). The yield of the synthesized P4C compound was 83%, with a melting point range of 224-225 °C. The yield of the synthesized 3-ACH compound was 62%, with a melting point range of 280-282 °C.

Fourier-Transform Infrared Spectroscopy (FT-IR)

The FTIR spectrum of P4C exhibited a distinctive absorption at 3066 cm^{-1} , indicating aromatic C-H bonds. The identified peak at 1696 cm^{-1} confirmed the existence of a carbonyl group associated with the aldehyde moiety in P4C. Additionally, the peaks in the range of $1600\text{-}1450\text{ cm}^{-1}$ corresponded to C=C and C=N bonds, consistent with the anticipated compound structure (Figure 2).

Similarly, 3-ACH, a derivative of P4C, displayed the characteristic peak for aromatic C-H bonds at 3066 cm^{-1} . Additional absorptions at 2959 cm^{-1} and 2869 cm^{-1} suggested aliphatic C-H bonds. The peak at 1656 cm^{-1} provided confirmation of the carbonyl group's existence, which is linked to the ketone group within the compound. Furthermore, the peaks in the $1600\text{-}1450\text{ cm}^{-1}$ range corresponded to C=C and C=N bonds present within the compound. Finally, the absorption peaks at 1532 cm^{-1} and 1388 cm^{-1} were attributed to the presence of nitro groups within the molecular structure (Figure 2) (16).

Nuclear Magnetic Resonance (NMR)

The $^1\text{H-NMR}$ spectrum of the P4C showed a singlet at 10.08 ppm, indicating the presence of the aldehyde proton (CHO), while the proton bonded to the carbon atom in the pyrazole ring (C5H) resonated as a singlet at 9.08 ppm. The aromatic protons exhibited a complex pattern of absorption, appearing as multiplets within the range of 7.97-7.42 ppm (Figure 3a). In the $^1\text{H-NMR}$ spectrum of 3-ACH, the proton attached to the pyrazole ring's carbon (C5H) appeared as a single signal at 7.99 ppm. Multiplet signals observed in the 7.98-7.40 ppm range were assigned to aromatic protons (Ar-H). The singlet at 5.57 ppm originated from the proton associated with the C9H carbon in the acridine ring. Singular signals at 2.66 and 2.61 ppm were assigned to protons at carbons C2-C7H and C4-C5H of the acridine ring, respectively. Furthermore, single peaks at 1.54 ppm and 1.13 ppm corresponded to methyl protons (CH₃) in the molecule (Figure 3b).

The $^{13}\text{C-NMR}$ spectrum of P4C displayed a signal at 183.73 ppm for the aldehyde carbon atom (C=O). The peaks at 168.19 ppm and 153.94 ppm were attributed to carbon 2 and 9 in the benzothiazole ring, respectively. The 12 peaks observed between 150.64 and 121.78 ppm were assigned to the aromatic carbons (Figure 3c). The $^{13}\text{C-NMR}$ spectrum of 3-ACH revealed a signal at 197.62 ppm, indicating the presence of the ketone (C=O) carbonyl within

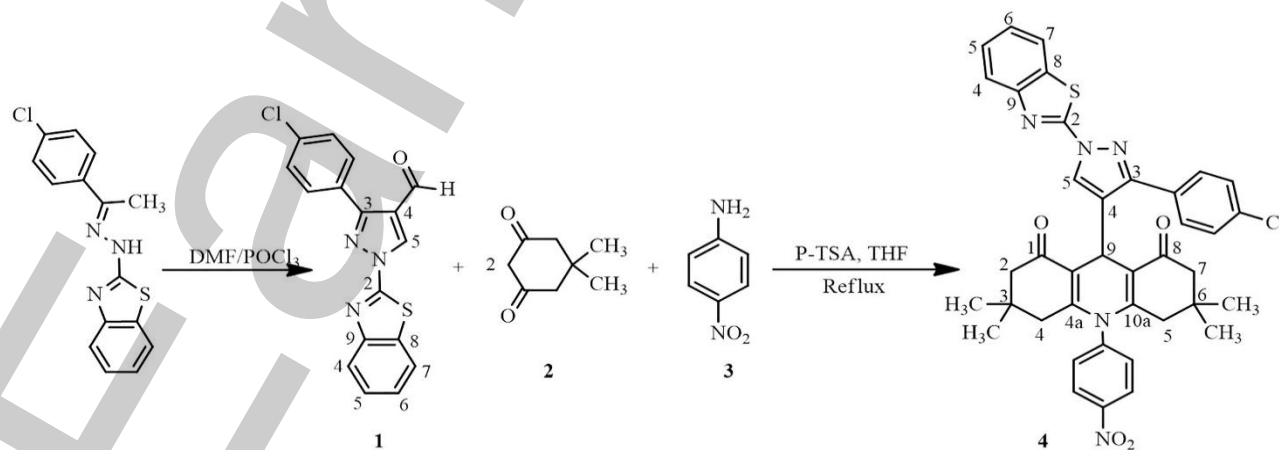


Figure 1. Synthesis of pyrazole-acridine derivative from hydrazone (1: P4C, 2: dimedone, 3: p-nitroaniline, 4: 3-ACH)

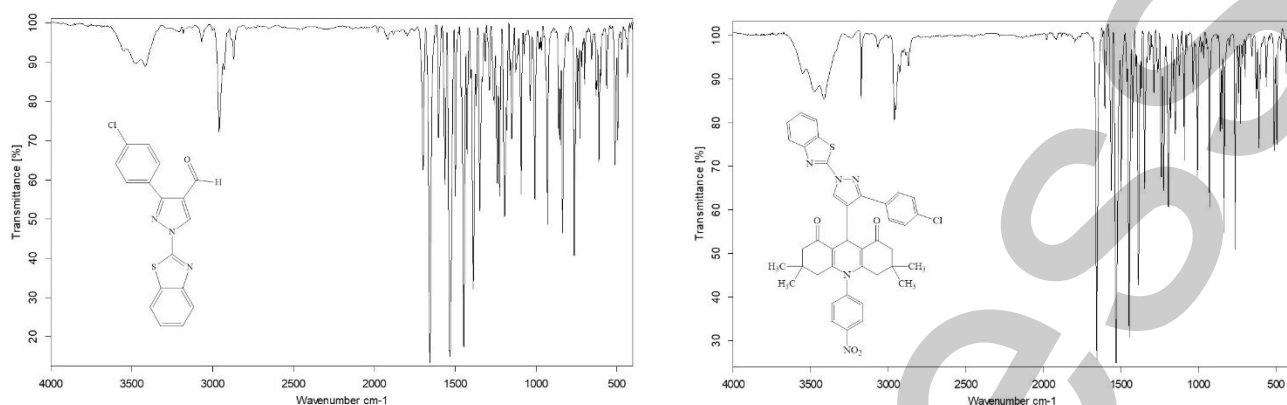


Figure 2. Fourier-transform infrared spectroscopy (FT-IR) spectrum of P4C and 3-ACH

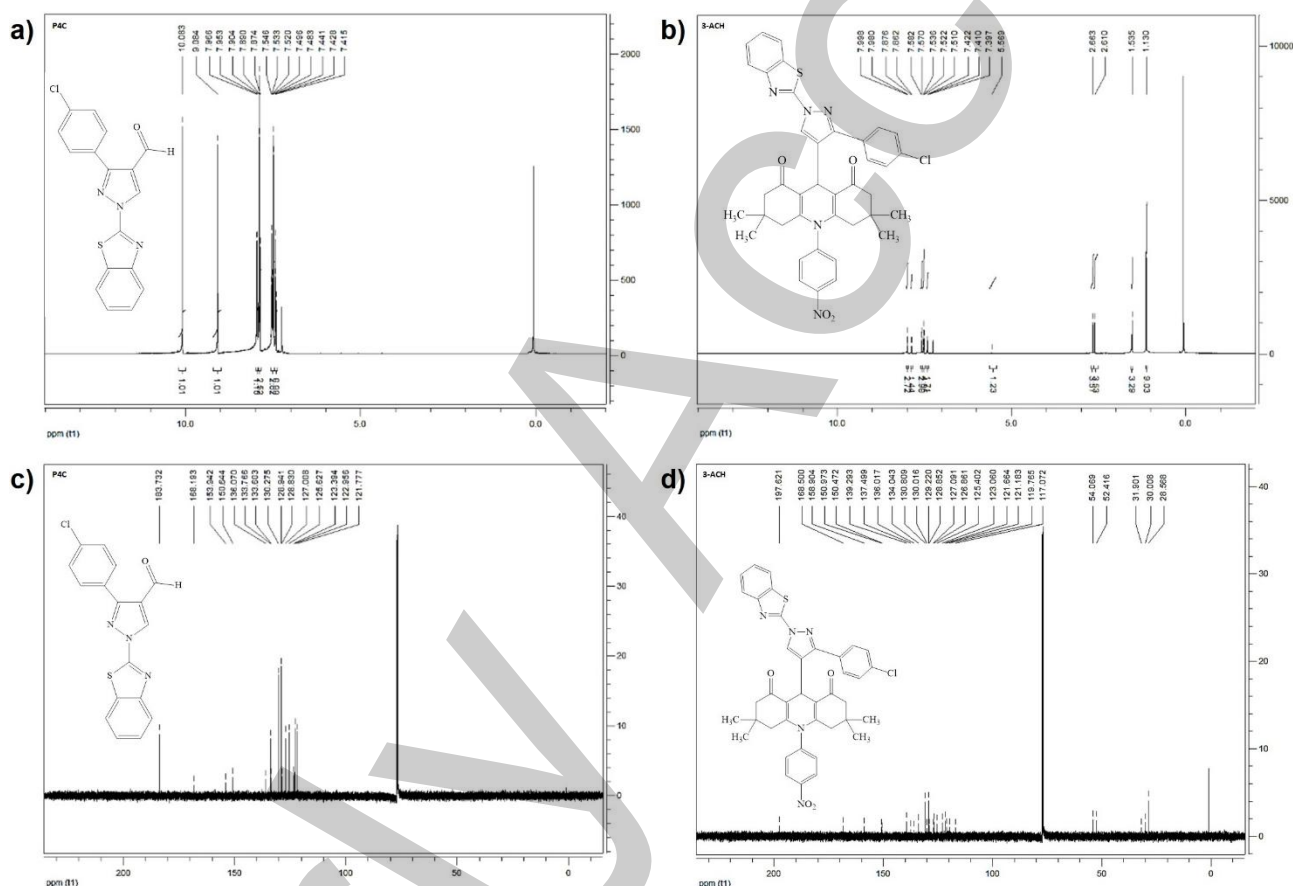


Figure 3. Nuclear magnetic resonance (NMR) spectra of synthesized compounds at 600 MHz and 150 MHz; **a)** ^1H -NMR spectrum of P4C, **b)** ^1H -NMR spectrum of 3-ACH, **c)** ^{13}C -NMR spectrum of P4C, **d)** ^{13}C -NMR spectrum of 3-ACH

the acridine ring. Signals at 168.50 ppm and 150.97 ppm were attributed to carbon 2 and carbon 9 in the benzothiazole ring, respectively. Furthermore, signals at 158.90 ppm and 158.70 ppm arose from the C4a and C10a carbons in the acridine ring, while the signal at 150.47 ppm denoted the carbon linked to the nitro atom (C-NO₂). Aliphatic carbon atoms were represented by signals at 54.07 ppm (C2 and C7), 52.42 ppm (C4 and C5), 31.90 ppm (C9), and 30.01 ppm (C3 and C6), all located in the acridine ring. Finally, the signal at 28.57 ppm in the spectrum originated from the methyl carbons within the molecule (Figure 3d) (17).

Mass Spectrometry (High-Performance Liquid Chromatography Quadrupole Time-of-Flight Mass Spectrometry, HPLC-Q-TOF/MS) Analysis

In the mass spectrum of P4C, the molecular ion peak was identified at m/z 338.33 [M-1], corresponding to the molecular formula C₁₇H₁₀ClN₃OS and possessing a mass of 338.02. The close agreement between the experimental and theoretical molecular ion peaks indicated a high level of purity for P4C (Figure 4). However, the theoretical mass of 3-ACH could not be directly confirmed due to its fragmentation during analysis. Therefore, elemental analysis was performed to further characterize 3-ACH (13).

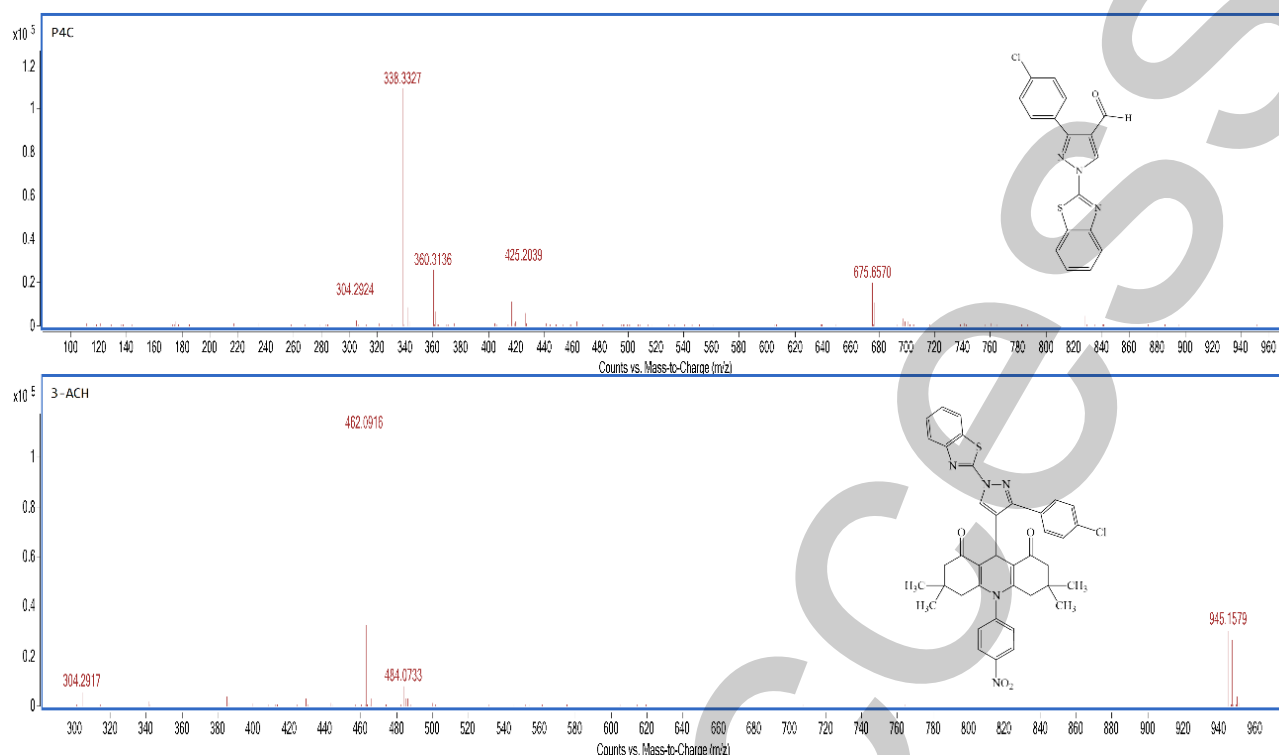


Figure 4. The mass spectrum of P4C and 3-ACH

Elemental Analysis

The results demonstrated close agreement between the calculated values and the experimental analysis for both P4C and 3-ACH (Table 1). These findings offer strong confirmation of the purity of the synthesized compounds and support the accuracy of their chemical structures.

Upon comprehensive evaluation of the combined FT-IR, NMR, mass spectra, and elemental analysis data, it can be concluded that the target compounds were successfully synthesized, with values consistent with previous research findings. This thorough analysis provides robust evidence regarding the successful synthesis and characterization of the compounds following established scientific knowledge.

Cell Viability

The application of 3-ACH for 12 hours resulted in a statistically significant decrease in cell viability rates of $94.54 \pm 2.50\%$ ($p=0.015$) and $94.33 \pm 1.84\%$ ($p=0.011$) at doses of $100 \mu\text{g/mL}$ and $150 \mu\text{g/mL}$, respectively. However, applying $50 \mu\text{g/mL}$ of 3-ACH for the same duration did not result in a significant decrease in cell viability rates ($98.28 \pm 4.69\%$, $p=0.718$) compared to the control group. While extending the exposure time to 24 hours, doses of $100 \mu\text{g/mL}$ ($89.89 \pm 7.63\%$, $p=0.002$) and $150 \mu\text{g/mL}$ ($90.53 \pm 2.88\%$, $p=0.004$) of 3-ACH continued to show a statistically significant reduction in cell viability compared to the control group, there was no statistically significant decrease observed when $50 \mu\text{g/mL}$ of 3-ACH

was applied for 24 hours ($98.37 \pm 1.67\%$, $p=0.903$). Additionally, both $100 \mu\text{g/mL}$ and $150 \mu\text{g/mL}$ doses showed significant decreases compared to the $50 \mu\text{g/mL}$ group ($p=0.011$ and $p=0.019$, respectively). Comparing the exposure times, the 24-hour application of 3-ACH at $100 \mu\text{g/mL}$ and $150 \mu\text{g/mL}$ resulted in a more substantial reduction in cell viability compared to the 12-hour application of 3-ACH at the same doses. After exposing the cells to 3-ACH for 48 hours, a notable and statistically significant reduction in cell viability was observed across all dosage levels when compared to the control group, $94.55 \pm 0.65\%$ for $50 \mu\text{g/mL}$, $95.18 \pm 1.41\%$ for $100 \mu\text{g/mL}$, and $95.28 \pm 2.57\%$ for $150 \mu\text{g/mL}$ (all $p < 0.001$, Figure 5). The overall effect of the 3-ACH treatment was significant at all time points ($p=0.004$ for 12 hours, $p < 0.001$ for both 24 and 48 hours, Table 2).

Table 1. P4C and 3-ACH elemental analysis

	P4C (C ₁₇ H ₁₀ ClN ₃ OS)		3-ACH (C ₃₉ H ₃₄ ClN ₅ O ₄ S)	
	Calculated	Found	Calculated	Found
% C	60.09	59.93	66.51	66.32
% H	2.97	3.01	4.87	4.90
% N	12.37	12.42	9.94	10.02
% S	9.44	9.47	4.55	4.61

Table 2. Cell survival rates (%) of SH-SY5Y cells treated with different doses of 3-ACH at different time points

Time	Control	3-ACH 50 $\mu\text{g/mL}$	3-ACH 100 $\mu\text{g/mL}$	3-ACH 150 $\mu\text{g/mL}$	p
12-hour	100.00 \pm 0.00	98.28 \pm 4.69	94.54 \pm 2.50 ^{***}	94.33 \pm 1.84 ^{***}	0.004
24-hour	100.00 \pm 0.00	98.37 \pm 1.67	89.89 \pm 7.63 ^{***}	90.53 \pm 2.88 ^{***}	<0.001
48-hour	100.00 \pm 0.00	94.55 \pm 0.65 ^{***}	95.18 \pm 1.41 ^{***}	95.28 \pm 2.57 ^{***}	<0.001

Values are presented as mean \pm standard deviation, *: different from control, **: different from 3-ACH 50 $\mu\text{g/mL}$, 1 symbol $p < 0.05$, 2 symbols $p < 0.005$, and 3 symbols $p < 0.001$

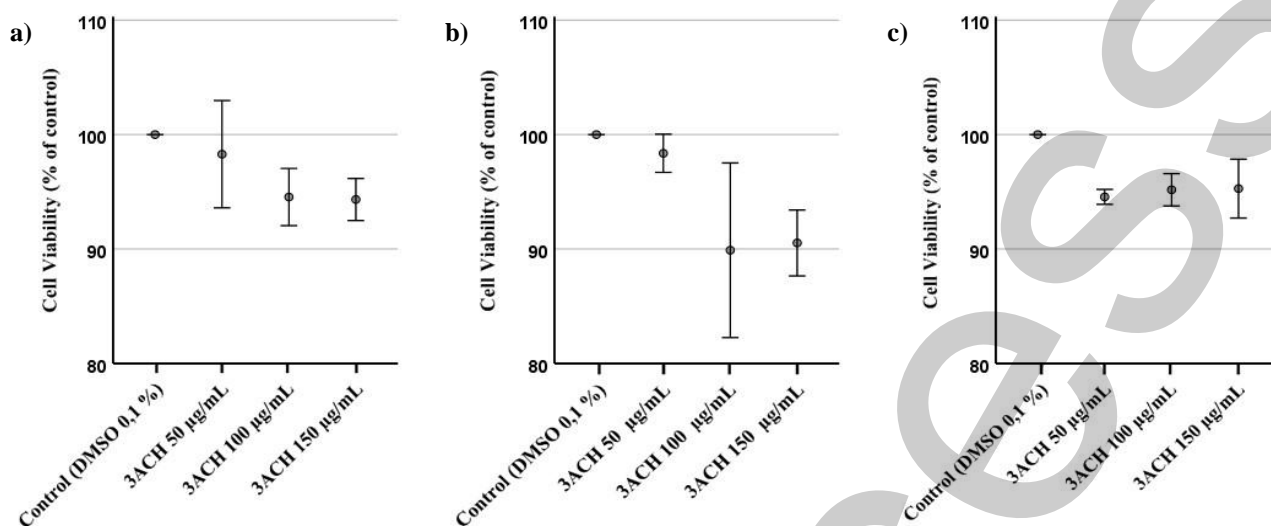


Figure 5. The cytotoxic impact of 3-ACH on SH-SY5Y cells was assessed at **a)** 12 hours, **b)** 24 hours, and **c)** 48 hours

3-ACH Stimulates Cell Death in SH-SY5Y Human Neuroblastoma Cells by Triggering Apoptosis

Immunofluorescence analysis revealed that BAX protein expression was significantly elevated in SH-SY5Y cells treated with 3-ACH (100 µg/mL) for 24 hours compared to untreated controls. Similarly, the expression levels of Caspase-3, -8, and -9 were markedly increased in treated cells compared to the control groups (Figure 6). These elevated levels of both intrinsic (BAX, Caspase-9) and extrinsic (Caspase-8) pathway proteins, together with the executioner caspase (Caspase-3), suggested comprehensive activation of apoptotic pathways.

DISCUSSION

Cancer is the uncontrolled movement of abnormal cells, which reduces the standard of living and is an important cause of death in both developed and developing countries. The core structure of pyrazole serves as the foundation for a class of medications employed in addressing various medical conditions. These conditions include cardiovascular diseases, neurological disorders, tumors, respiratory ailments, endocrine disorders, and metabolic abnormalities.

In recent years, research interest in pyrazole derivatives has been increasing due to their diverse biological activities. Currently, there are 34 pyrazole-based therapeutic drugs under investigation in clinical practice or clinical trials (18). Pyrazole is a significant heterocyclic structure with a potent pharmacological profile and can serve as a crucial pharmacophore in the drug discovery procedure, particularly for the development of anti-cancer and anti-inflammatory drugs (19). The pyrazolic analogue with different pharmacophoric subunits has been tested in numerous cancer cell lines, including neuroblastoma. The lethal effect of bis(pyrazolyl)alkanes co-synthesized with Pd (II) dichloride and diacetate complexes on SH-SY5Y has been demonstrated using the 3-(4,5-dimethylthiazol-2-yl)-2,5-diphenyltetrazolium bromide (MTT) cytotoxicity test. However, their cytotoxic impact was less pronounced compared to cisplatin (20). A novel series of 1,2,4-oxadiazoles incorporating 1,2,3-triazole-pyrazoles was synthesized, and cytotoxicity tests were performed on cancer cell lines, including A549 (lung cancer), DU-145 and

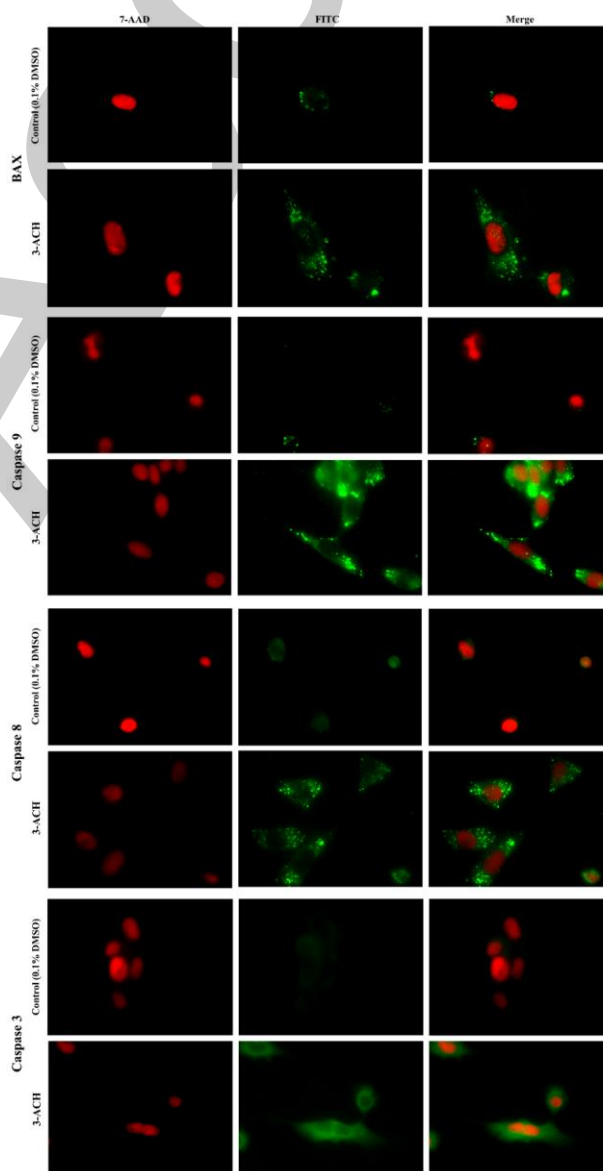


Figure 6. Expression level of the BAX, Caspase-3, -8, and -9 proteins in SH-SY5Y cells (x100). Cell nuclei were stained using the 7-AAD dye, producing a red signal, the BAX, Caspase-3, -8, and -9 proteins were detected using a FITC-labeled antibody, represented by a green signal

PC3 (prostate cancer), and MCF-7 (breast cancer) human cancer cell lines. Many of the synthesized compounds showed activity against all cell lines, while some demonstrated a more potent cytotoxic effect (21). In the study by Akhtar et al. (22), specific pyrazole-pyrazoline hybrid derivatives targeting the COX-2 enzyme were synthesized. They demonstrated strong anticancer potential against A549, SiHa (cellosaurus cancer cell line), HepG2 (hepatocellular carcinoma), and COLO205 (colon cancer) cell lines, as evidenced by the MTT assay (with IC50 values of approximately 4.94 μ M, 4.94 μ M, 2.09 μ M, and 4.86 μ M, respectively). Given the specificity of these compounds towards the COX-2 enzyme, it can be inferred that they exerted their anticancer effects through COX-2 inhibition.

Acridine, a crystalline compound discovered by Graebe and Caro in 1870 from coal tar, has many uses, including medicine and industry. Acridine has been the subject of research with its antibacterial, antiparasitic, antiviral, and antimalarial properties. The anticancer effect of acridine derivatives has been investigated due to interactions with DNA and DNA-related enzymes, topoisomerase II, and telomerase (23,24). Hybrid compounds of 9-aminoacridine and artemisinin-acridine were synthesized and the cytotoxic and apoptotic activity of HepG2 and SH-SY5Y were evaluated against CHO cells (Chinese hamster ovary cells), and both acridine and artemisinin pharmacophores showed hepatotoxicity and neurotoxicity (25).

Recent studies have highlighted the therapeutic potential of combining the pyrazole and acridine pharmacophores. Hu et al. (26) demonstrated that pyrazoloacridine exhibits synergistic cytotoxicity when combined with conventional anticancer agents like doxorubicin, etoposide, and topotecan, particularly in drug-resistant tumor cells. Their research showed that these combinations could effectively overcome drug resistance mechanisms. Additionally, Adjei (12) reported that pyrazoloacridine represents a novel class of anticancer agents with distinct advantages, including activity against solid tumors, effectiveness in hypoxic conditions, and ability to target drug-resistant cells. Notably, pyrazoloacridine maintains its activity against cells that are resistant to other agents due to P-glycoprotein overexpression or topoisomerase deficiency. Building on these promising findings, phase 2 clinical studies have been conducted evaluating pyrazole-acridine derivatives in breast and ovarian cancer (27,28). In a pioneering study, Sugaya et al. (29) demonstrated significant inhibition of HeLa S3 cell proliferation in vitro and remarkable suppression of P388 leukemia and sarcoma 180 solid tumors in vivo using novel pyrazole-acridine derivatives. Notably, these compounds exhibited superior antitumor activity at lower doses compared to adriamycin.

Our results indicate that 3-ACH holds promise as a potential anticancer agent for targeting SH-SY5Y human neuroblastoma cells. The cytotoxic effects of pyrazole derivatives on neuroblastoma cells have been demonstrated in the literature. In our study, we similarly confirmed the anticancer properties of the pyrazole-acridine compounds that we synthesized on neuroblastoma cells. Furthermore, we elucidated the underlying apoptotic mechanism of cell death through immunostaining. Apart from its cytotoxic impact, we additionally noticed that the administration of 3-ACH activated several apoptosis-associated proteins,

such as BAX, Caspase-9, -8, and -3. These proteins have well-established roles in both the intrinsic and extrinsic apoptotic pathways, which are tightly regulated mechanisms of programmed cell death frequently disrupted in cancer cells.

Apoptosis is a complex process with two main pathways: the intrinsic (mitochondrial) pathway and the extrinsic (cell surface receptor-mediated) pathway. When these apoptotic processes work in balance, they contribute to healthy tissue homeostasis, being a natural part of the cell's life cycle (30). Compared to the control group, there was an increase in the synthesis of proteins involved in the intrinsic pathway components, BAX and Caspase-9. Additionally, the synthesis of Caspase-8, an extrinsic pathway component, and Caspase-3, which plays a role in both intrinsic and extrinsic pathways, significantly increased. These results indicate that 3-ACH may exert its cytotoxic effect by activating both intrinsic and extrinsic pathways.

We have synthesized a novel pyrazole-acridine derivative using a four-step synthetic process and characterized its structure using FT-IR, NMR, HPLC-Q-TOF/MS, and elemental analysis techniques. This development is particularly significant given the current limitations of chemotherapy, which despite being the prevailing approach in cancer treatments, suffers from several drawbacks including high toxicity, side effects, costly nature, and limited targeting specificity. Our findings suggest that pyrazole-acridine hybrids may offer a promising alternative therapeutic approach for cancer treatment, with the potential for enhanced efficacy and improved selectivity. However, it is important to acknowledge certain limitations of our study and address future research directions. The current investigation primarily focused on in vitro analyses, and while these results are promising, they represent only the initial steps in understanding the therapeutic potential of 3-ACH. Several critical aspects require further investigation: First, additional experimental approaches, such as intracellular calcium imaging and Western blot analysis, are needed to provide stronger validation of the apoptotic pathways we observed. Second, the compound's ability to cross the blood-brain barrier, which is crucial for treating neuroblastoma, remains to be determined. Third, whether 3-ACH acts as a prodrug requiring metabolic activation or functions directly in its current form is yet to be established. To address these questions, comprehensive in vivo studies will be necessary to assess both the compound's efficacy and safety profile in animal models. Additionally, investigating potential synergistic effects with existing chemotherapeutic agents could provide valuable insights for combination therapy approaches. These future investigations would significantly enhance our understanding of 3-ACH's therapeutic potential and guide its development as an anticancer agent.

CONCLUSIONS

Our research illustrates that 3-ACH has cytotoxic effects on SH-SY5Y human neuroblastoma cells, which are dependent on both the dosage and duration of exposure. Additionally, we noted activation of apoptosis-associated proteins, such as BAX, Caspase-3, -8, and -9, upon exposure to 3-ACH. These proteins are crucial in the intrinsic and extrinsic apoptotic pathways, which are tightly regulated

mechanisms of programmed cell death that are often disrupted in cancerous cells. The stimulation of these proteins indicates that 3-ACH possesses the capability to trigger apoptosis, serving as the underlying mechanism responsible for its cytotoxic impact on SH-SY5Y human neuroblastoma cells. Further investigations are necessary to elucidate the precise mechanisms through which 3-ACH acts on neuroblastoma cancer cells.

Ethics Committee Approval: Since our study was not an experimental study including human or animal subject, ethics committee approval was not required.

Conflict of Interest: None declared by the authors.

Financial Disclosure: None declared by the authors.

Acknowledgments: We would like to express our sincere gratitude to the Biotechnology Institute of Ankara University for providing the necessary resources for conducting cell culture and biochemical analyses. We appreciate Assoc. Dr. Erkan YILMAZ for giving the SH-SY5Y human neuroblastoma cancer cell line.

Author Contributions: Idea/Concept: YK, ME, FE, MD; Design: YK, ME, FE, MD; Data Collection/Processing: YK, ME, FE, HY, RK, MD; Analysis/Interpretation: YK, ME, HY, RK, MD; Literature Review: YK, ME, FE; Drafting/Writing: YK, ME, FE; Critical Review: YK, ME, FE, MD.

REFERENCES

- Nandurkar D, Danao K, Rokde V, Shivhare R, Mahajan U. Pyrazole scaffold: Strategies toward the synthesis and their applications. In: Kumari P, Patel AB, editors. Strategies for the synthesis of heterocycles and their applications. London, UK: IntechOpen; 2022. p15-38.
- Kumar V, Kaur K, Gupta GK, Sharma AK. Pyrazole containing natural products: Synthetic preview and biological significance. *Eur J Med Chem.* 2013;69:735-53.
- Karrouchi K, Radi S, Ramli Y, Taoufik J, Mabkhot YN, Al-Aizari FA, et al. Synthesis and pharmacological activities of pyrazole derivatives: A review. *Molecules.* 2018;23(1):134.
- Nitulescu GM. Quantitative and qualitative analysis of the anti-proliferative potential of the pyrazole scaffold in the design of anticancer agents. *Molecules.* 2022;27(10):3300.
- Costa RF, Turones LC, Cavalcante KVN, Rosa Júnior IA, Xavier CH, Rosseto LP, et al. Heterocyclic compounds: Pharmacology of pyrazole analogs from rational structural considerations. *Front Pharmacol.* 2021;12:666725.
- Alfei S, Brullo C, Caviglia D, Piatti G, Zorzoli A, Marimpietri D, et al. Pyrazole-based water-soluble dendrimer nanoparticles as a potential new agent against staphylococci. *Biomedicines.* 2021;10(1):17.
- Kornis GI. Pyrazoles, pyrazolines, and pyrazolones. In: Kirk-Othmer encyclopedia of chemical technology. 3rd ed. New York: John Wiley & Sons; 2000. p.436-53.
- National Center for Biotechnology Information. PubChem compound summary for CID 9215, Acridine. 2023. [Cited: 2024 Jul 23]. Available from: <https://pubchem.ncbi.nlm.nih.gov/compound/Acridine>
- Prasher P, Sharma M. Medicinal chemistry of acridine and its analogues. *Medchemcomm.* 2018;9(10):1589-618.
- Varakumar P, Rajagopal K, Aparna B, Raman K, Byran G, Gonçalves Lima CM, et al. Acridine as an anti-tumour agent: A critical review. *Molecules.* 2022;28(1):193.
- Gackowski M, Szewczyk-Golec K, Pluskota R, Koba M, Mađra-Gackowska K, Woźniak A. Application of multivariate adaptive regression splines (MARSplines) for predicting antitumor activity of anthrapyrazole derivatives. *Int J Mol Sci.* 2022;23(9):5132.
- Adjei AA. Current status of pyrazoloacridine as an anticancer agent. *Invest New Drugs.* 1999;17(1):43-8.
- Elmusa M, Elmusa S, Mert S, Kasımoğulları R, Türkan F, Atalar MN, et al. One-pot three-component synthesis of novel pyrazolo-acridine derivatives and assessment of their acetylcholinesterase inhibitory properties: An in vitro and in silico study. *J Mol Struct.* 2023;1274(1):134553.
- Küçükbağrıaçık Y, Dastouri MR, Elmusa M, Elmusa F, Yılmaz H, Kasımoğulları R. Evaluation of the potential anticancer activity of pyrazole-acridine derivative synthesis on SKBR-3 human breast cancer cell line. *KÜ Tıp Fak Derg.* 2024;26(1):76-85. Turkish.
- Kucukbagriacik Y, Dastouri M, Yilmaz H, Altuntas EG. The apoptotic effect of the Lycopodium clavatum extracts on MCF-7 human breast cancer cells. *Med Oncol.* 2023;40(10):289.
- Nandiyanto ABD, Oktiani R, Ragadhita R. How to read and interpret FTIR spectroscopy of organic material. *Indonesian J Sci Technol.* 2019;4(1):97-118.
- Gunawan R, Nandiyanto ABD. How to read and interpret ¹H-NMR and ¹³C-NMR spectrums. *Indonesian J Sci Technol.* 2021;6(2):267-98.
- Zhai H, Zhang S, Ampomah-Wireko M, Wang H, Cao Y, Yang P, et al. Pyrazole: An important core in many marketed and clinical drugs. *Russ J Bioorg Chem.* 2022;48(6):1175-89.
- Alam MJ, Alam O, Naim MJ, Nawaz F, Manaihiya A, Imran M, et al. Recent advancement in drug design and discovery of pyrazole biomolecules as cancer and inflammation therapeutics. *Molecules.* 2022;27(24):8708.
- Di Nicola C, Marchetti F, Pettinari C, Pettinari R, Brisdelli F, Crucianelli M, et al. Synthesis and characterization of a new alkyne functionalized bis(pyrazolyl)methane ligand and of its Pd(II) complexes: Evaluation of their in vitro cytotoxic activity. *Inorganica Chim Acta.* 2017;455(2):677-82.
- Mohan G, Sridhar G, Laxminarayana E, Chary MT. Synthesis and biological evaluation of 1,2,4-oxadiazole incorporated 1,2,3-triazole-pyrazole derivatives as anticancer agents. *Chem Data Coll.* 2021;34:100735.
- Akhtar W, Marella A, Alam MM, Khan MF, Akhtar M, Anwer T, et al. Design and synthesis of pyrazole-pyrazoline hybrids as cancer-associated selective COX-2 inhibitors. *Arch Pharm (Weinheim).* 2021;354(1):e2000116.

23. Varakumar P, Rajagopal K, Aparna B, Raman K, Byran G, Gonçalves Lima CM, et al. Acridine as an anti-tumour agent: A critical review. *Molecules*. 2022;28(1):193.
24. Rupar JS, Dobričić VD, Aleksić MM, Brborić JS, Čudina OA. A review of published data on acridine derivatives with different biological activities. *Kragujevac J Sci*. 2018;40:83-101.
25. Joubert JP, Smit FJ, du Plessis L, Smith PJ, N'Da DD. Synthesis and in vitro biological evaluation of aminoacridines and artemisinin-acridine hybrids. *Eur J Pharm Sci*. 2014;56:16-27.
26. Hu Y, Krishan A, Nie W, Sridhar KS, Mayer LD, Bally M. Synergistic cytotoxicity of pyrazoloacridine with doxorubicin, etoposide, and topotecan in drug-resistant tumor cells. *Clin Cancer Res*. 2004;10(3):1160-9.
27. Plaxe SC, Blessing JA, Bookman MA, Creasman WT. Phase II trial of pyrazoloacridine in recurrent platinum-sensitive ovarian cancer: a Gynecologic Oncology Group study. *Gynecol Oncol*. 2002;84(1):32-5.
28. Ramaswamy B, Mrozek E, Kuebler JP, Bekaii-Saab T, Kraut EH. Phase II trial of pyrazoloacridine (NSC#366140) in patients with metastatic breast cancer. *Invest New Drugs*. 2011;29(2):347-51.
29. Sugaya T, Mimura Y, Shida Y, Osawa Y, Matsukuma I, Ikeda S, et al. 6H-pyrazolo[4,5,1-de]acridin-6-ones as a novel class of antitumor agents. Synthesis and biological activity. *J Med Chem*. 1994;37(7):1028-32.
30. Jan R, Chaudhry GE. Understanding apoptosis and apoptotic pathways targeted cancer therapeutics. *Adv Pharm Bull*. 2019;9(2):205-18.